International Journal of Multidisciplinary Studies and Innovative Technologies

e-ISSN: 2602-4888
dergipark.org.tr/en/pub/ijmsit
Research Article

2024, 8 (1), 35-39
DOI: 10.36287/ijmsit.8.1.6
Received: June 2, 2024; Accepted: July 1, 2024

Feedback Linearized Model Predictive Control of a Two Link Robot Arm

Mehmet Karahan[1*]

[1*]*Electrical and Electronics Engineering Department, TOBB University of Economics and Technology, Ankara, Türkiye (mehmetkarahan@etu.edu.tr) (ORCID: 0000-0002-5828-497X)*

Abstract **–** Nowadays, robotic arms are widely used in industry. Robotic arms are used in applications such as pick and place, arc welding, spot welding, packaging, machine maintenance, and material handling. Robot arms are used extensively especially in the automotive industry. The use of robotic arms reduces the need for labor, reduces costs and reduces work accidents. As the importance of robotic arms increases with the development of industry, the problem of controlling robot arms has also gained importance. In this study, modeling of a 2-link robot arm and model predictive controller (MPC) design were carried out. The nonlinear dynamic model of the robotic arm is linearized through feedback linearization. MATLAB and Simulink programs were used to model the linearized robotic arm. MPC controller design was carried out for the linearized robot arm model and thus the movements of the robot arm could be controlled. The simulations performed revealed that the designed MPC successfully controlled the robotic arm.

Keywords *– model predictive control, feedback linearization, mathematical model, manipulator dynamics, robot kinematics*

Citation: Karahan, M. (2024). Feedback Linearized Model Predictive Control of a Two Link Robot Arm. International Journal of Multidisciplinary Studies and Innovative Technologies, 8(1): 35-40.

I. Introduction

With the development of the industry, the role of robotic arms in production processes has increased. Robot arms can successfully perform repetitive, dangerous and power-requiring tasks for humans [1], [2], [3].

Robotic arms have multi-degree of freedom movement and have advanced software and hardware [4], [5], [6]. For this reason, it becomes important to control robotic arms successfully in order to avoid occupational accidents and to prevent the production process from being disrupted [7], [8].

Different control techniques have been used to control robotic arms [9]. However, PID controllers have been used more widely than others [10]. The simple structure of the PID controller and easy adjustment of its parameters lead to its widespread use [11]. Renuka et al. modeled a 3 degrees of freedom (DOF) robot manipulator and designed a PID controller [12]. Jawad et al. designed an artificial neural network (ANN) optimized PID controller for a robot arm [13]. Das et al. developed a fuzzy fractional order PID controller for a robot arm and they used MATLAB program for simulations [14]. Sutyasadi et al. designed a cascaded PID controller for a three axis articulated robotic arm [15].

Some of the researchers used LQR controller because of its simplicity, robustness and flexibility [16]. Song et al. modeled a 2 DOF robot manipulator and designed an optimum LQR controller [17]. Ortega-Vidal et al. conducted a comparative study for a 2 DOF robot arm. They compared optimal LQR controller and LQR predictive controller [18]. Choubey et al. proposed a LQR based PID controller for a 3 DOF robot arm. They used MATLAB program for simulations [19].

In this study, the control of a two-link robotic arm was carried out with a feedback linearized MPC controller. First of all, the equations of two connected robotic arms were derived. These equations were linearized with feedback linearization to obtain a linear robot arm model. MPC controller was designed to control the movements of the linearized robotic arm. The robot arm was modeled and the MPC controller was designed using MATLAB and Simulink programs. Simulations have shown that the MPC controller works successfully.

II. Modeling of The Robot Arm

In this study, a 2-degree-of-freedom robotic arm was used. The schematic representation of the used robotic arm is given in Fig. 1.

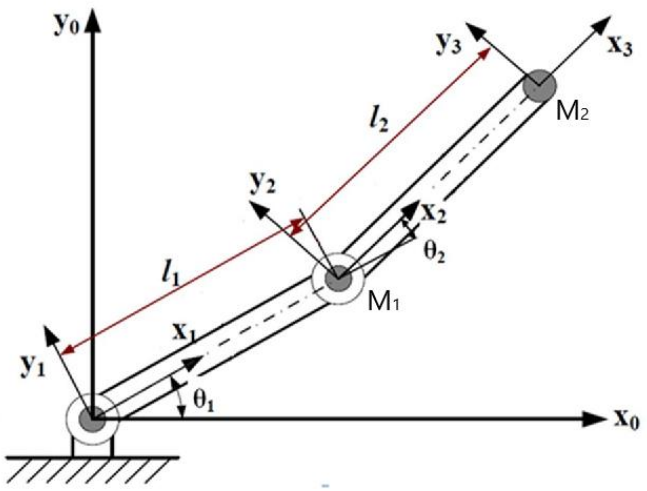

Fig. 1. 2-link robot arm

In Fig. 1, l_1 and l_2 show the lengths of the robot arm. θ_1 and θ_2 show the angles of the robotic arm. M_1 indicates the mass of the first link and M_2 indicates the mass of the second link.

The dynamic model of the robotic arm is calculated based on kinetic and potential energies. This dynamic model is calculated using the dynamic geometric model given by the following formulas.

$$x = L_1\sin(\theta_1) + L_2\sin(\theta_1+ \theta_2) \quad (1)$$
$$y = L_1\cos(\theta_1) + L_2\cos(\theta_1+ \theta_2) \quad (2)$$

Using equations (1) and (2), the kinetic energy equation of the 2-link robotic arm is found as follows.

$$E = \frac{1}{2}(M_1 + M_2)L_1^2\dot{\theta}_1^2 + \frac{1}{2}M_2L_2^2\dot{\theta}_1^2 + M_2L_2^2\dot{\theta}_1\dot{\theta}_2 + \frac{1}{2}M_2L_2^2\dot{\theta}_2^2 + M_2L_1L_2(\dot{\theta}_1\dot{\theta}_2 + \dot{\theta}_1^2)\cos(\theta_2) \quad (3)$$

Potential energy is represented in (4)

$$U = M_1gL_1\cos(\theta_1) + M_2g(L_1\cos(\theta_1) + L_2\cos(\theta_1+\theta_2)) \quad (4)$$

The motion equations of the robot can be found using the Lagrange equation. Lagrange's equation is given in (4).

$$L = E-U \quad (5)$$

To calculate the equations of motion, the Euler-Lagrange equation is used, which is based on the partial derivative of the kinetic and potential energy properties of mechanical systems and is defined in equation (6).

$$\tau = \frac{d}{dt}\left(\frac{\partial L}{\partial \dot{\theta}_i}\right) - \left(\frac{\partial L}{\partial \theta_i}\right) \quad (6)$$

L is Lagrangian of the motion and τ represents torque. Torque vector is represented in (7).

$$\tau = [\tau_1\ \tau_2]^T \quad (7)$$

Dynamic model of the robotic arm with 2 DOF is represented in (8).

$$\begin{cases} M(\theta)\ddot{\theta} + C(\theta,\dot{\theta}) + G(\theta) = \tau \\ Y = \theta \end{cases} \quad (8)$$

In the above equations θ is the joint variable vector and is represented in (9).

$$\theta = [\theta_1\ \theta_2]^T \quad (9)$$

Y is the output vector. G(θ) represents the gravity torques vector, C(θ, $\dot{\theta}$) is vector of Coriolis and centrifugal forces and M(θ) is the inertia matrix. G(θ) is given in (10).

$$G(\theta)=\begin{bmatrix} -(M_1 + M_2)gL_1\sin(\theta_1) - M_2gL_2\sin(\theta_1 + \theta_2) \\ -M_2gL_2\sin(\theta_1 + \theta_2) \end{bmatrix} \quad (10)$$

C(θ, $\dot{\theta}$) vector is presented in (11).

$$C(\theta,\dot{\theta}) = \begin{bmatrix} -M_2L_1L_2(2\dot{\theta}_1\dot{\theta}_2 + \dot{\theta}_1^2)\sin(\theta_2) \\ -M_2L_1L_2\dot{\theta}_1\dot{\theta}_2\sin(\theta_2) \end{bmatrix} \quad (11)$$

M(θ) inertia matrix is shown in (12)

$$M(\theta) = \begin{bmatrix} D_1 & D_2 \\ D_3 & D_4 \end{bmatrix} \quad (12)$$

D_1, D_2, D_3, D_4 constants are given in (13).

$$\begin{cases} D_1 = (M_1 + M_2)L_1^2 + M_2L_2^2 + 2M_2L_1L_2cos(\theta_2) \\ D_2 = M_2L_2^2 + M_2L_1L_2\cos(\theta_2) \\ D_3 = D_2 \\ D_4 = M_2L_2^2 \end{cases} \quad (13)$$

III. Control Structure

In this section, a model predictive controller is developed for the 2 DOF robot arm. Firstly, feedback linearization control is used to linearize model. Secondly, a model predictive controller is designed for the linear robot arm model.

A. Feedback Linearization Control

With this technique, the nonlinear dynamics of the system are made linear and linear control techniques become applicable to control the system.

The output Y is differentiated until the control input τ is obtained. In this case, the control input τ is obtained in the second derivative of Y. This equation is given in (14)

$$\ddot{Y} = \ddot{\theta} = M(\theta)^{-1}(- C(\theta,\dot{\theta}) - G(\theta) + \tau) = v \quad (14)$$

In the above equation, v is a synthetic control vector. This vector is defined in (15).

$$v = [v_1\ v_2]^T \quad (15)$$

Using (7), feedback linearization control is obtained in (16).

$$\tau = M(\theta)v + C(\theta,\dot{\theta}) + G(\theta) \quad (16)$$

By using the control law given in (16), linearization of the system in (8) is achieved and linear system for each joint is obtained as in (17) and (18). In below equations, p is Laplace variable.

$$\frac{\theta_1(p)}{v_1(p)} = \frac{1}{p^2} \quad (17)$$

$$\frac{\theta_2(p)}{v_2(p)} = \frac{1}{p^2} \quad (18)$$

B. Model Predictive Control

After the linearization of the nonlinear robot arm model, the below decoupled linear systems are obtained.

$$\ddot{\theta}_1 = v_1 \quad (19)$$

$$\ddot{\theta}_2 = v_2 \quad (20)$$

The above system could be rewritten in the state space form as in (21). v_1 is the synthetic control of the first joint of the robot arm and Y is output.

$$\begin{cases} \dot{x}_1(t) = x_2(t) \\ \dot{x}_2(t) = v_1(t) \\ Y(t) = x_1(t) \end{cases} \quad (21)$$

Secondly, relationship between x and θ states are presented in (22).

$$[x_1\ x_2]^T = [\theta_1\ \dot{\theta}_1]^T \quad (22)$$

Firstly, an MPC controller was developed for the first connection of the robot arm. A controller is developed in a similar way for the second connection. In the time interval [t t+h], $v_1(t) = v_1$ is assumed. h is horizon time of prediction. Using the (21), prediction model is found as in (23)

$$\begin{cases} \dot{\theta}_1(t+h) = v_1 h + \dot{\theta}_1(t) \\ \theta_1(t+h) = \frac{1}{2} v_1 h^2 + \dot{\theta}_1(t) h + \theta_1(t) \end{cases} \quad (23)$$

The given reference angle of the first link θ_{1d}, the proposed one-horizon time quadratic cost function to stabilize the system is given in (24).

$$J = e_1^2(t+h) + p\dot{e}_1^2(t+h) \quad (24)$$

The predicted angle error is given in (25).

$$e_1(t+h) = \theta_{1d} - \theta_1(t+h) \quad (25)$$

The predicted velocity error is given in (26).

$$\dot{e}_1(t+h) = 0 - \dot{\theta}_1(t+h) \quad (26)$$

In the above equations, h is horizon time and p is weight factor. Substituting the prediction model (23) in (24) and minimizing J criteria with respect to v_1 value, the MPC controller is obtained. The obtained MPC controller is given in (27).

$$v_1(t) = k_3\theta_{1d} - k_1\theta_1(t) - k_2\dot{\theta}_1(t) \quad (27)$$

k_1,k_2 and k_3 control gains are presented in below equations.

$$k_1 = \frac{2}{h^2+4p} \quad (28)$$

$$k_2 = \frac{2h^2+4p}{h^3+4ph} \quad (29)$$

$$k_2 = \frac{2}{h^2+4p} \quad (30)$$

MPC controller coefficients are represented in Table 1.

Table 1. MPC controller coefficients

Parameter	Definition	Value
k_1	Controller Gain	15.99
k_2	Controller Gain	5.65
k_3	Controller Gain	15.99
p	Weight Factor	1.14 x 10^{-9}
h	Horizon Time	0.35 s

IV. Control Structure

In this section, simulations made using MATLAB/Simulink are included. The parameters of the robotic arm used in this study are shown in Table 2.

Table 2. Robot arm parameters

Parameter	Definition	Value
M_1	Mass of the first link	1 kg
M_2	Mass of the second link	1 kg
L_3	Length of the first link	1 m
L_2	Length of the second link	1 m
g	Gravity	9.81 m/s^2

The model of the robot arm and MPC controller designed in Simulink is shown in Fig. 2.

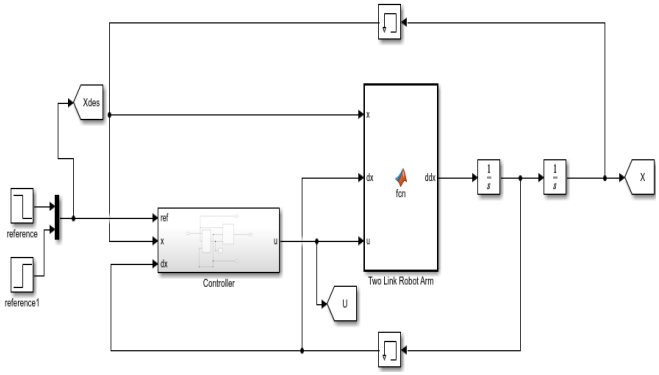

Fig. 2. Simulink model of the robot arm and MPC controller

Initial conditions and desired conditions of the robot arm is given in Table 3.

Table 3. Initial and desired conditions of the robot arm

Parameter	Definition	Value
$\theta_1(0)$	Initial angle of the first link	π/2
$\theta_2(0)$	Initial angle of the second link	-π/2
θ_{1d}	Desired angle of the first link	-π/2
θ_{2d}	Desired angle of the second link	π/2

Figure 3 to Fig. 7 show simulations of the robotic arm. In simulations, the angle value is in radians and the time value is in seconds. Simulation of the $\theta_1$angle is shown in Fig. 3. As can be seen from Fig. 3, the MPC controller reaches the desired angle value in a short time.

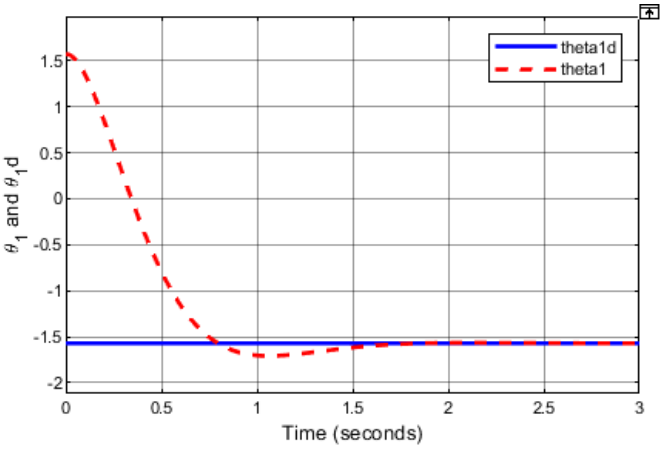

Fig. 3. Simulation of the θ_1 angle

Figure 4 represents the θ_2 angle simulation. As seen in Fig. 4, the MPC controller reaches the desired angle value in a short time.

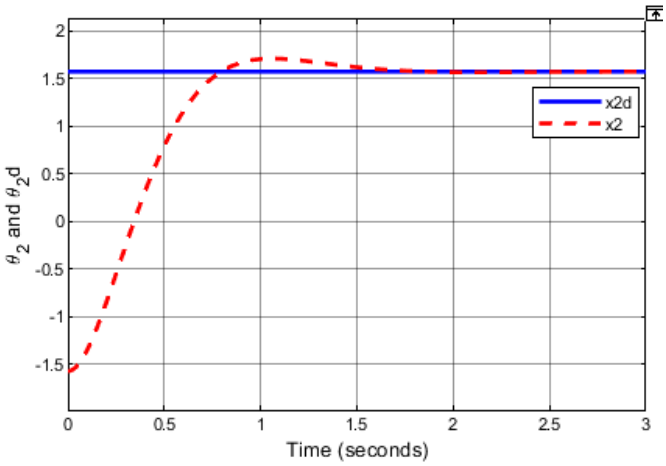

Fig. 4. Simulation of the θ_2 angle

Torques of the robot arm's links are given in Fig. 5.

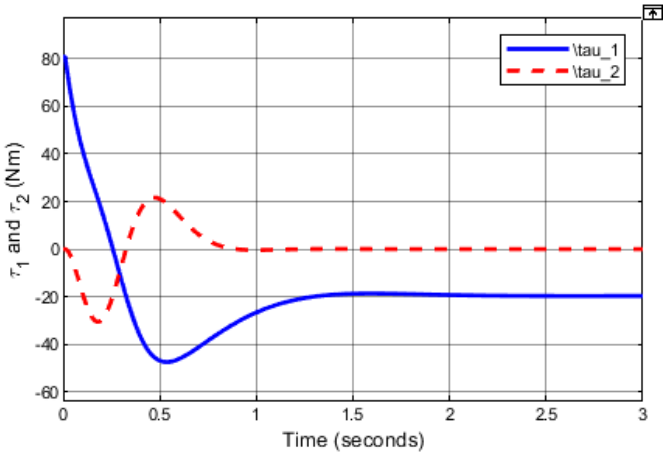

Fig. 5. Torques of the robot arm's links

Simulation of the synthetic control vector is represented in Fig. 6. As seen in Fig. 6, the synthetic controls reach zero when the end effector of the robotic arm reaches its target.

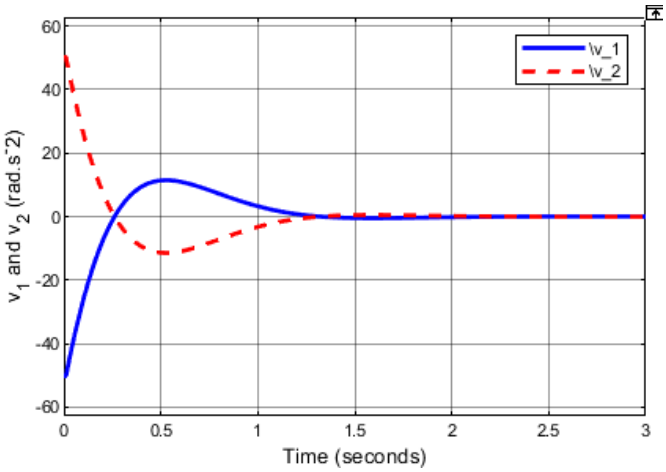

Fig. 6. Synthetic control vector

The error graph for the 1st and 2nd lines of the robot arm is as shown in Fig. 7. As can be seen in Fig. 7, the error value goes to 0 for both robot arm links. In this case, it turns out that the robot arm is controlled by MPC flawlessly.

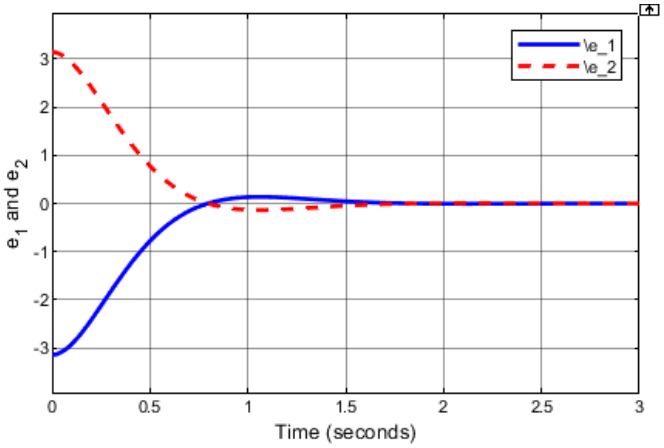

Fig. 7. Error graph of the robot arm's links

V. Conclusion

In this study, feedback linearized model predictive control of a two-link robot arm was implemented. First of all, the equations of the robotic arm were derived and the dynamic model was created. Then, the robot arm model was linearized with feedback linearization. MPC controller was developed to control the linearized robot arm model. The linear robotic arm and MPC controller were created using MATLAB/Simulink. Simulations were made for the angles, synthetic vector, torque values and error values of the robotic arm. In the simulations, it was seen that the MPC controller achieved the desired angle values in a very short time. It has been observed that synthetic vector values and error values go to zero in a short time. Thus, it has been confirmed that the developed MPC controller successfully controls the two-link robot arm.

References

[1] I. Daniyan, K. Mpofu, B. Ramatsetse, A. Adeodu, "Design and simulation of a robotic arm for manufacturing operations in the railcar industry," Procedia Manufacturing, vol. 51, pp. 67-72, 2020.

[2] J. -D. Lee, W. -C. Li, J. -H. Shen and C. -W. Chuang, "Multi-robotic arms automated production line," 2018 4th International Conference on Control, Automation and Robotics (ICCAR), Auckland, New Zealand, 2018, pp. 26-30.

[3] R. Wright, S. Parekh, R. White, D. P. Losey, "Safely and autonomously cutting meat with a collaborative robot arm," Scientific Reports, vol. 14(1), pp. 299, 2024.

[4] Y. Tian, W. Feng, M. Ouyang, H. Bian and Q. Chen, "A positioning error compensation method for multiple degrees of freedom robot arm based on the measured and target position error", Adv. Mech. Eng., vol. 14, no. 5, pp. 1-13, May 2022.

[5] A. Talli and V. K. Meti, "Design simulation and analysis of a 6-axis robot using robot visualization software", IOP Conf. Series: Materials Science and Engineering, pp. 1-9, 2020.

[6] W. Montalvo, J. Escobar-Naranjo, C. A. Garcia and M. V. Garcia, "Lowcost automation for gravity compensation of robotic arm", in Applied Sciences vol. 10(11), pp. 3823, 2020.

[7] M. Javaid, A. Haleem, R. P. Singh, S. Rab and R. Suman, "Significant applications of Cobots in the field of manufacturing", Cognitive Robotics, vol. 2, pp. 222-233, 2022.

[8] J.-C. Liao, S.-H. Chen, Z.-Y. Zhuang, B.-W. Wu and Y.-J. Chen, "Designing and Manufacturing of Automatic Robotic Lawn Mower", Processes, vol. 9, pp. 358, 2021.

[9] J. D. J. Rubio et al., "Modified Linear Technique for the Controllability and Observability of Robotic Arms," in IEEE Access, vol. 10, pp. 3366-3377, 2022

[10] M. Bi, "Control of Robot Arm Motion Using Trapezoid Fuzzy Two-Degree-of-Freedom PID Algorithm", Symmetry, vol. 12, pp. 450-455, 2020.

[11] M. Karahan and C. Kasnakoglu, "Modeling a Quadrotor Unmanned Aerial Vehicle and Robustness Analysis of Different Controller

Designs under Parameter Uncertainty and Noise Disturbance", Journal of Control Engineering and Applied Informatics, vol. 23, no. 4, pp. 13-24, December 2021.

[12] K. Renuka, N. Bhuvanesh, J. R. Catherine, “Kinematic and dynamic modelling and PID control of three degree-of-freedom robotic arm,” In Advances in Materials Research: Select Proceedings of ICAMR, pp. 867-882, 2021.

[13] A. T. Jawad, N. S. Ali, A. N. Abdullah and N. H. Alwash, "Design of Adaptive Controller for Robot Arm Manipulator Based on ANN with Optimized PID by IWO Algorithm," 2021 International Conference on Advanced Computer Applications (ACA), Maysan, Iraq, 2021, pp. 107-111.

[14] S. Das, N. Dey, “Fuzzy Fractional Order PID Controller Design for Single Link Robotic Arm Manipulator,” Industrial Control Systems, 2024, pp. 203-230.

[15] P. Sutyasadi, M. B. Wicaksono and D. Maneetham, "Improvement Control of a Three Axis Articulated Robotic Arm Using PID Cascade Control," 2023 11th International Conference on Cyber and IT Service Management (CITSM), Makassar, Indonesia, 2023, pp. 1-4.

[16] M. Karahan and C. Kasnakoglu, "LQR Control and Observer Design of a Magnetically Suspended Ball," 2022 International Congress on Human-Computer Interaction, Optimization and Robotic Applications (HORA), Ankara, Turkey, 2022, pp. 1-4.

[17] T. Song, Y. Li, S. Ma, H. Li, “LQR Optimal Control Method Based on Two-Degree-of Freedom Manipulator,” In International Conference on Neural Computing for Advanced Applications, pp. 477-488, 2022.

[18] A. Ortega–Vidal, F. Salazar–Vasquez and A. Rojas–Moreno, "A comparison between optimal LQR control and LQR predictive control of a planar robot of 2DOF," 2020 IEEE XXVII International Conference on Electronics, Electrical Engineering and Computing (INTERCON), Lima, Peru, 2020, pp. 1-4.

[19] C. Choubey and J. Ohri, "Tuning of LQR-PID controller to control parallel manipulator", Neural Comput. Appl., vol. 34, no. 4, pp. 3283-3297, 2022.